

# Stochastic finite element-based reliability analysis of space frames

Vissarion Papadopoulos & Manolis Papadrakakis†

*Institute of Structural Analysis and Seismic Research, National Technical University Athens, Athens 15773, Greece*

In the present paper the weighted integral method in conjunction with Monte Carlo simulation is used for the stochastic finite element-based reliability analysis of space frames. The limit state analysis required at each Monte Carlo simulation is performed using a non-holonomic step-by-step elasto-plastic analysis based on the plastic node method in conjunction with efficient solution techniques. This implementation results in cost effective solutions both in terms of computing time and storage requirements. The numerical results presented demonstrate that this approach provides a realistic treatment for the stochastic finite element-based reliability analysis of large scale three-dimensional building frames. © 1997 Elsevier Science Ltd.

## 1 INTRODUCTION

The theory and methods of stochastic analysis have been developed significantly during the last ten years and have been documented in an increasing number of publications. Considerable progress in applying stochastic process theory to the area of structural engineering has made it possible to achieve higher levels of reliability. This leads to safety measures that design engineers have to take into account due to the inherent probabilistic nature of the design parameters, such as material properties, geometry and/or loading conditions. Stochastic analysis involves the estimation of the response variability and/or reliability of a stochastic system defined as a structural system that possesses uncertainties in its material and/or geometric properties. Although from a theoretical point of view the field has reached a stage where the developed methodologies are becoming widespread, from a computational point of view, serious obstacles have been encountered in practical implementations.

Analytic solutions to the problem are restricted to simple linear elastic structures under static loads while most of the current research work is focused in obtaining numerical solutions that are more appropriate for handling realistic problems.<sup>1</sup> Stochastic finite element methods (SFEM) belong to this category. SFEM approaches are based on the representation of stochastic fields as a series of random variables and various methodologies have been developed in order to achieve this objective.<sup>2–8</sup> The response statistics are

then obtained using one of the stochastic finite element methods: the perturbation or Taylor expansion based methods,<sup>2–4</sup> the weighted integral method,<sup>7,8</sup> the Neumann expansion method<sup>9,10</sup> and the polynomial chaos expansion method.<sup>5,6</sup> Perturbation methods have, however, a limited range of applicability since they can only be accurate for small values of variability of the stochastic properties, while it has been found that they are insufficient to deal with the variation of time history response due to an uncertain natural frequency.<sup>11</sup> In addition, these methods require, in order to be accurate, fine element meshes so that the element size is a fraction of the correlation distance of the stochastic field involved in the problem. The weighted integral method is based on a weighted integral representation of the stochastic field. The main advantage of this method is the calculation of the response variability of stochastic systems with great accuracy even when using relatively coarse finite element meshes. Furthermore, for beam elements, the accuracy of this method is independent of the chosen mesh.<sup>8,12</sup> The improved Neumann expansion method proposed in Ref. 10 is a robust and computationally efficient procedure compared to the standard Neumann expansion method,<sup>9</sup> while the methods that rely on the Karhunen–Loeve decomposition of the stochastic field coupled with either a Neumann expansion scheme or a polynomial chaos expansion<sup>5,6</sup> also behave well for relatively coarse finite element sizes and a wide range of random fluctuations.

First and second-order reliability methods that have been developed to estimate structural reliability<sup>13–17</sup> lead to elegant formulations requiring the definition of a differentiable failure function. For small-scale problems

†Author to whom correspondence should be addressed.

these type of methods prove to be very efficient, but for large-scale problems Monte Carlo simulation (MCS) methods under certain conditions may be more suitable.<sup>18</sup> The basic MCS is simple to use, but for typical structural reliability problems the computational effort involved becomes excessive because of the enormous sample size and the CPU time required for each Monte Carlo run. The use of Monte Carlo simulation (MCS) based on SFEM approaches has the major advantage that accurate solutions can be obtained for any problem whose deterministic solution is known either numerically or analytically. In fact, it is the only method available to solve certain stochastic problems involving non-linearities, dynamic loading, stability effects, parametric excitations, etc. The disadvantage of the standard MCS is that it is usually extremely computationally demanding. This problem is even more pronounced in the case of stochastic finite element-based reliability analysis of complex structures, where the limit state functions are not available in close forms, since each Monte Carlo simulation requires the performance of a full non-linear analysis.

In the present paper, the weighted integral method in conjunction with Monte Carlo simulation is used for the stochastic finite element-based reliability analysis of space frames. The limit state analysis required at each Monte Carlo simulation is performed using a non-holonomic step-by-step elastoplastic analysis based on the plastic node method<sup>19–21</sup> for space frames in conjunction with efficient solution techniques developed in Refs 22 and 23. The implementation of some recent developments in hybrid solution techniques, particularly suitable for three-dimensional applications, results in cost effective solutions both in terms of computing time and storage requirements. The numerical results presented demonstrate that this approach provides a realistic treatment for the stochastic finite element-based reliability analysis of large-scale three-dimensional building frames.

## 2 STOCHASTIC FINITE ELEMENT ANALYSIS OF SPACE FRAMES

### 2.1 The weighted integral method

The weighted integral method has been applied in Refs 7 and 8 to formulate the stochastic element stiffness matrix for a 2-D beam element. In this section, the corresponding stochastic stiffness matrix of a 3-D beam element is derived.<sup>10</sup>

For a 3-D beam element with 12 degrees of freedom per node the modulus of elasticity is assumed to vary randomly along the element length according to

$$E^{(e)}(x) = E_0[1 + f^{(e)}(x)] \quad (1)$$

where  $E_0$  is the mean value of the modulus of elasticity and  $f^{(e)}(x)$  is a one-dimensional univariate (1D–1V)

zero mean homogeneous stochastic field independently assigned for each member of the structure.

In order to avoid the possibility of obtaining non-positive values of the elastic modulus,  $f^{(e)}(x)$  is assumed to be bounded according to

$$-0.80 < f^{(e)}(x) < 0.80 \quad (2)$$

These bounds are implemented as follows: any digitally generated sample function that has at least one of its values out of the bounds, is automatically discarded.

The stochastic element stiffness matrix is given by

$$K^{(e)} = \int_0^{L^{(e)}} B^{(e)T} D^{(e)} B^{(e)} dx \quad (3)$$

where

$$D^{(e)} = E^{(e)}(x) \begin{bmatrix} A^{(e)} & 0 & 0 & 0 \\ 0 & I_3^{(e)} & 0 & 0 \\ 0 & 0 & I_2^{(e)} & 0 \\ 0 & 0 & 0 & \frac{J^{(e)}}{2(1+\nu)} \end{bmatrix} \quad (4)$$

$B^{(e)}$  is the matrix containing the derivatives of the shape functions and  $A^{(e)}$ ,  $I_2^{(e)}$ ,  $I_3^{(e)}$ ,  $J^{(e)}$  are the cross-sectional area the cross-sectional moments of inertia for weak and major axis and the torsional modulus, respectively.  $L^{(e)}$  and  $\nu$  are the length of the element and the Poisson ratio, respectively.

Performing integration with respect to  $x$ , the stochastic stiffness matrix  $K^{(e)}$  may be expressed as

$$K^{(e)} = K_0^{(e)} + X_0^{(e)} \Delta K_0^{(e)} + X_1^{(e)} \Delta K_1^{(e)} + X_2^{(e)} \Delta K_2^{(e)} \quad (5)$$

or

$$K^{(e)} = K_0^{(e)} + \Delta K^{(e)} \quad (6)$$

$K_0^{(e)}$  and  $\Delta K^{(e)}$  denote the stationary and the fluctuating part of the stochastic element stiffness matrix, respectively.  $X_0^{(e)}$ ,  $X_1^{(e)}$  and  $X_2^{(e)}$  are the so-called weighted integrals which are random variables defined as

$$X_0^{(e)} = \int_0^{L^{(e)}} f^{(e)}(x) dx \quad (7)$$

$$X_1^{(e)} = \int_0^{L^{(e)}} x f^{(e)}(x) dx \quad (8)$$

$$X_2^{(e)} = \int_0^{L^{(e)}} x^2 f^{(e)}(x) dx \quad (9)$$

$K_0$  is the mean value of  $K^{(e)}$  since the weighted integrals have zero mean and  $\Delta K_0$ ,  $\Delta K_1$ ,  $\Delta K_2$  are deterministic matrices the definition of which can be found in Appendix A.

### 2.2 Representation of stochastic field

Since Monte Carlo simulation (MCS) techniques are

used to calculate the reliability of the stochastic structural system, it is necessary to digitally generate sample functions of the 1D–1V stationary Gaussian zero mean homogeneous stochastic field  $f(x)$ . This is done using the spectral representation method<sup>24</sup> taking advantage of the fast Fourier transform (FFT) technique in order to reduce the computational effort of the simulation. This is achieved using the formula

$$f^{(j)}(p\Delta x) = \text{Re} \left\{ \sum_{n=0}^{M-1} B_n^j e^{inp(2\pi/M)} \right\}, \quad (10)$$

$$p = 0, 1, \dots, M-1$$

$$j = 1, 2, \dots, NSIM$$

where  $\text{Re}$  indicates the real part,  $M$  defines the number of points at which  $f(x)$  process is realized along the element length,  $NSIM$  is the number of samples to be generated.  $B_n^j$  is given by

$$B_n^j = \sqrt{2} A_n e^{i\phi_n^{(j)}}, \quad n = 0, 1, \dots, M-1 \quad (11)$$

where  $\phi_n^{(j)}$  represents the  $j$ th realization of the independent random phase angles uniformly distributed in the range  $[0-2\pi]$ ,  $A_n$  is defined as

$$A_n = (2S_{ff}(n\Delta k)\Delta k)^{1/2}, \quad n = 0, 1, \dots, M-1 \quad (12)$$

and

$$\Delta k = \frac{k_u}{N} \quad (13)$$

$k_u$  is the upper cut-off wave number and  $N$  is the number of intervals in the discretization of the spectrum.  $S_{ff}$  is the two-sided power spectral density function defined as

$$S_{ff} = \frac{1}{4} \sigma_f^2 b_f^3 k^2 e^{-b_f k} \quad (14)$$

where  $\sigma_f$  denotes the standard deviation of the stochastic field,  $b_f$  denotes the parameter that influences the shape of the spectrum and hence the scale of the correlation and  $k = n\Delta k$ .

The weighted integrals are computed numerically using eqns (7)–(9), while the stochastic field  $f^{(e)}(x)$  is simulated using eqn (10). It should be mentioned that the weighted integrals can be generated directly from their known covariance matrix rather than going through the stochastic field as proposed by Wall and Deodatis.<sup>12</sup> The latter approach is more efficient compared to the adopted procedure. The comparison of the computational efficiency of the proposed methods, however, is not affected by this overhead in the computation of the weighted integrals, since this is identical for all methods used in this study.

### 3 STOCHASTIC FINITE ELEMENT-BASED RELIABILITY ANALYSIS

In reliability analysis, MCS is often employed when the

analytical solution is not attainable and the failure domain cannot be expressed or approximated by an analytical form. This is mainly the case in problems of complex nature with a large number of basic variables where all the other methods are not applicable.

Expressing the limit state function as  $G(X)$ , where  $X = (X_1, X_2, \dots, X_n)$  is the vector of the basic random variables and/or random fields, following the law of large numbers, an unbiased estimator of the probability of failure is given by<sup>25</sup>

$$\bar{p}_f = \frac{1}{NSIM} \sum_{j=1}^{NSIM} I(X_j) \quad (15)$$

where  $I(X_j)$  is an indicator defined as

$$I(X_j) = \begin{cases} 1 & \text{if } G(X_j) \leq 0 \\ 0 & \text{if } G(X_j) > 0 \end{cases} \quad (16)$$

Subsequently, using eqn (10) a large number of sample functions ( $NSIM$ ) may be produced for each element of the structure generating a set of stochastic stiffness matrices as well as  $NSIM$  independent random load variables of a specific probability density function. Then, the failure function is computed for each sample  $X_j$ . If  $G(X_j) \leq 0$  a successful simulation is counted. The Monte Carlo estimate of  $p_f$  can then be expressed in terms of sample mean as

$$\bar{p}_f = \frac{N_H}{NSIM} \quad (17)$$

where  $N_H$  is the number of successful simulations.

### 4 LIMIT ELASTOPLASTIC ANALYSIS

In this work the reliability analysis connected to a structural failure criterion of framed structures is examined. The failure criterion is considered to be the formation of a mechanism. The adopted incremental non-holonomic first-order step-by-step limit analysis is based on the generalized plastic node concept proposed in Ref. 19. The non-linear yield surface is approximated by a multi-faceted surface as shown in Fig. 1(a), while the linear equilibrium equations at each load step are solved using the preconditioned conjugate gradient method.<sup>20,21</sup>

Under the assumption of concentrated plasticity all plastic deformations are confined to zero length plastic zones at the two ends of the member, leaving elastic the part of the member between the two plastic nodes. The materials are assumed to be elastic–perfectly plastic and the structural response is in the range of small displacements. The tangent elasto-plastic stiffness matrix used for the limit state analysis may be expressed as

$$K_{ep} = K_e - K_e \Phi \{ \Phi^T K_e \Phi \}^{-1} \Phi^T K_e \quad (18)$$

in which  $K_{ep}$  is the elasto-plastic element stiffness matrix,  $K_e = K_0 + \Delta K$  is the elastic stochastic element stiffness matrix, and  $\Phi$  is the gradient vector of the multi-faceted

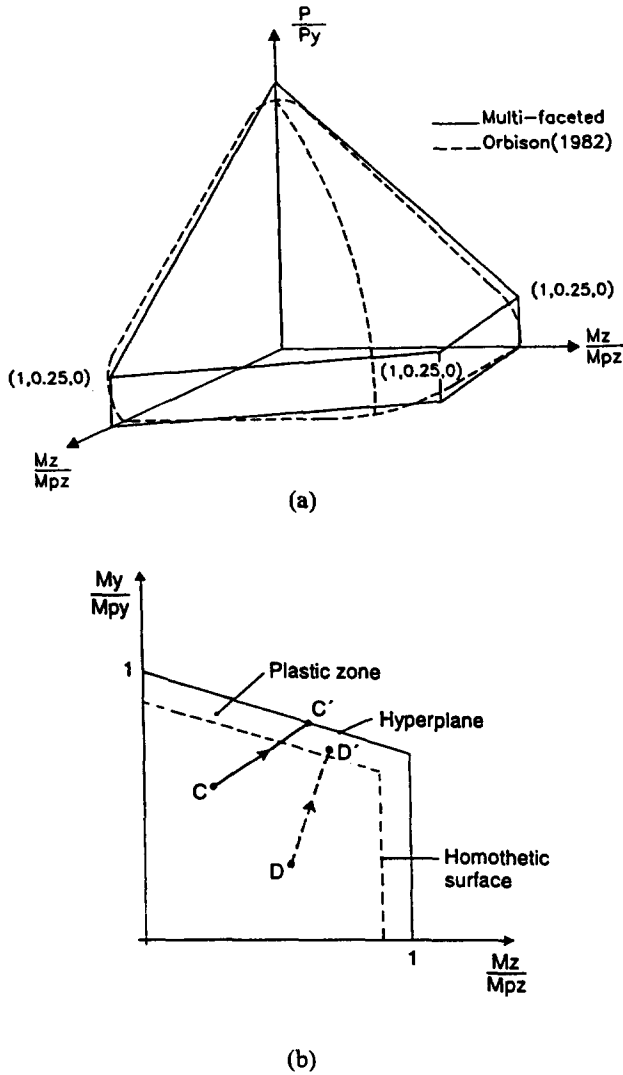


Fig. 1. (a) Yield surface and multi-faceted approximation. (b) The trace of the plastic zone on the  $M_y - M_z$  plane and the activation of new yield modes.

surface at the force point where a member-end initiates the plastic behaviour. In this study, the yield surface proposed in Ref. 26 is approximated by a piece-wise linear multi-faceted surface. For an efficient computer implementation a second internal yield surface of similar orientation (*homothetic*) and close to the first one (see Fig. 1(b)) is introduced in order to avoid unnecessary analysis steps.<sup>21</sup> The original yield surface together with its homothetic create a zone with well-defined dimensions where the activation of a yield mode starts as soon as the force point of an element-end crosses the internal surface (path CC' in Fig. 1(b)). This implementation allows the activation of more than one yield mode within the same load step (path DD' in Fig. 1(b)). In our application, the distance between the two yield surfaces is defined by a tolerance criterion  $\epsilon_s$  which controls the activation of a yield mode. Thus, instead of a force point oscillating around a sharp corner of the multi-faceted yield surface for a number of steps without any advancement on the loading path, simultaneous

formation of more than one plastic nodes will change significantly the global stiffness characteristics forcing the oscillating point to move towards a new direction away from the corner of oscillation.

## 5 SOLUTION PROCEDURES

### 5.1 The preconditioned conjugate gradient method

The incremental limit analysis of space frames, described in the previous section, requires a number of subsequent linear solutions in which the overall stiffness matrix is slightly modified from one solution to the other. The total number of solutions corresponds to the total number of load increments required for the structure to become a mechanism. The change of stiffness from one step to the other is only due to the contribution of the elasto-plastic stiffness matrices of the elements with the newly formed plastic nodes. These special features of the problem make the preconditioned conjugate gradient method (PCG) very attractive for the solution of the linear problem at each load increment. The PCG is established as the more attractive iterative procedure for solving linear problems resulting from the finite element discretization. An important factor in the success of this method in solving large-scale finite element equations is the preconditioned technique used to improve the ellipticity of the coefficient matrix. This typically consists of replacing the original system  $Ku = f$  by the equivalent system

$$R^{-1}Ku = R^{-1}f \quad (19)$$

where  $R$  is the transformation or preconditioning matrix which is an approximation to  $K$  and it is non-singular. The PCG algorithm, based on the most efficient conjugate gradient version with respect to computational labour, storage requirements and accuracy is defined as follows for the untransformed variables:

$$\begin{aligned} a_m &= \frac{(r^{(m)}, z^{(m)})}{(d^{(m)}, Kd^{(m)})} \\ u^{(m+1)} &= u^{(m)} + a_m d^{(m)} \\ r^{(m+1)} &= r^{(m)} + a_m Kd^{(m)} \\ \text{if } \|r^{(m+1)}\| / \|f\| &\leq e \text{ then stop} \\ z^{(m+1)} &= R^{-1}r^{(m+1)} \\ a_m &= \frac{(r^{(m+1)}, z^{(m+1)})}{(r^{(m)}, z^{(m)})} \\ d^{(m+1)} &= -z^{(m+1)} + a_m d^{(m)} \\ \text{with } r^{(0)} &= Ku^{(0)} - f, z^{(0)} = R^{-1}r^{(0)}, d^{(0)} = z^{(0)} \end{aligned} \quad (20)$$

At the heart of the PCG iterative procedure for solving  $Ku = f$  is the determination of the residual vector and the selection of the preconditioning matrix. The accuracy achieved and the computational labour of the method is largely determined by how these two parameters are selected. A study performed in Ref. 23 revealed that the computation of the residual vector from its defining formula  $r^{(m)} = Ku^{(m)} - f$  with an explicit or a first-order differences matrix-vector multiplication  $Ku^{(m)}$  offers no improvement in the accuracy of the computed results. In fact, it was found that, contrary to previous recommendations, the calculation of the residuals by the recursive expression of algorithm (20) produces a more stable and well-behaved iterative procedure. Based on this observation, a mixed precision PCG implementation is proposed in which all computations are performed in single precision, except for double precision computation of the matrix vector multiplication occurring during the recursive evaluation of the residual vector. This implementation is a robust and reliable solution procedure even for handling large and ill-conditioned problems, while it is also computer storage-effective. It was also proved to be more cost-effective, for the same storage demands, than double precision calculations.<sup>22,23</sup>

The preconditioned matrix  $R$  has to be selected appropriately so that the eigenvalues  $R^{-1}K$  are spread over a much narrower range than those of  $K$ . For the type of problems considered in this study the elastic stochastic part of the stiffness matrix is taken as the initial preconditioning matrix. The diagonal and triangular factor of the  $LDL^T$  factorization of  $K_e = K_0 + \Delta K$  are stored in double or in single precision arithmetic, while the frequency of updating the preconditioning matrix due to the elasto-plastic contributions of the newly formed plastic nodes is controlled by the ratio of the time required for one full factorization to the time required for one PCG iteration. If the number of iterations at one step of the limit analysis becomes larger than this ratio, then the preconditioner is updated by refactorizing the current elasto-plastic matrix  $K_{ep}$ .

## 5.2 The Neumann-CG Method (NCG)

In order to improve the quality of the preconditioning matrix used in the PCG method, a Neumann series expansion is implemented for the calculation of the preconditioned vector  $z$  of algorithm (20).<sup>10</sup> The preconditioning matrix is now defined as the complete stochastic elastoplastic stiffness matrix  $K_{ep} = K_e + \Delta K_{ep}$ , where  $\Delta K_{ep}$  is the matrix containing the changes of the elastic matrix due to the successive formation of plastic nodes, but the solution for  $z$  is now performed approximately using a truncated Neumann series expansion. Thus, the preconditioned vector  $z$  of the

PCG algorithm is obtained at each iteration by

$$z = z_0 - z_1 + z_2 - z_3 + \dots \quad (21)$$

where  $z_0$  is given by

$$z_0 = K_e^{-1}r \quad i = 1, 2, \dots \quad (22)$$

and  $z_i$  is obtained by

$$K_e z_i = \Delta K_{ep} z_{i-1} \quad i = 1, 2, \dots \quad (23)$$

In the above expressions the superscript  $(m+1)$  has been dropped for clarity. The solution of eqn (23) is performed in double or single precision arithmetic.

The incorporation of the Neumann series expansion in the preconditioned step of the PCG method can be seen from the PCG point of view as an improvement on the quality of the preconditioning matrix by computing a better approximation to the solution of  $u = (K_0 + \Delta K)^{-1}f$  than the one provided by the preconditioning matrix  $K_e$ .

## 5.3 The complete Cholesky $LDL^T$ factorization

In this study, the proposed solution technique is compared to a conventional direct method for the solution of the linear equations at each load step. One of the most efficient direct solutions is considered to be the  $LDL^T$  Cholesky factorization of the stiffness matrix stored in skyline form. Since for large-scale 3-D frames the solution phase at each load step represents a significant investment in computing effort, a simple modification in the factorized process is implemented in our case resulting in significant savings in computing time. During the factorization phase, the alterations to the factorized stiffness matrix are confined to the bottom right-hand corner starting from the first node with a change in the stiffness matrix due to the plastic node formation at the end of one or more elements connected to that node. Consequently, the time-consuming factorization part need not be repeated from the beginning but only the steps after the smallest degree of freedom which is affected by the changes in the stiffness matrix and downwards. Thus, the elasto-plastic stiffness matrix is not refactorized at each load step but is partially refactorized starting with the least degree of freedom affected by plastic node formations. This technique is referred to as a modified complete factorization.

## 6 NUMERICAL TESTS

Two test examples have been carried out in order to test the performance of the methods previously described. A compact storage scheme is used for PCG and NCG methods to store the stiffness matrix. Non-zero terms are stored in a real vector, while the corresponding

column numbers are stored in an integer vector of equal length. An additional integer vector with length equal to the number of equations is used to record the start of each row inside the compact scheme. The extra storage for the conjugate gradient method is  $5n$  real positions, where  $n$  corresponds to the number of degrees of freedom. The direct MCS procedure with the complete Cholesky  $LDL^T$  factorization is handled either with two skyline storage routines for  $K$  and  $L$  (version a) or with a compact storage for  $K$  and a skyline storage for  $L$  (version b) in double precision arithmetic. In estimating the computer storage it is assumed that integers are stored as  $\text{INTEGER} \times 2$  or  $\text{INTEGER} \times 4$  according to their maximum possible values, and the floating point variables as  $\text{REAL} \times 4$  or  $\text{REAL} \times 8$  according to the accuracy of computation, single or double precision, respectively.

### Example 1

The first test example is the six storey space frame shown in Fig. 2. The yield strength of all elements is taken as 250 MPa. The lengths of beams and columns are 7.32 and 3.66 m, respectively. The loads consist of a  $19 \text{ KN m}^{-2}$  mean gravity load on all floor levels and a mean lateral load of 109 kN applied to each node in the front elevation in the negative  $z$  direction. The number of equations is 180 and the half bandwidth of the stiffness matrix is 41. The modulus of elasticity is considered to be a 1D-1V zero mean homogeneous stochastic field. Two sets of sample functions were prepared: the first with a standard deviation of 0.10 and the second with 0.20, while for both sets the value of the parameter  $b_f$  was assumed to be 1. The load-displacement curve is also shown in Fig. 2 for the mean

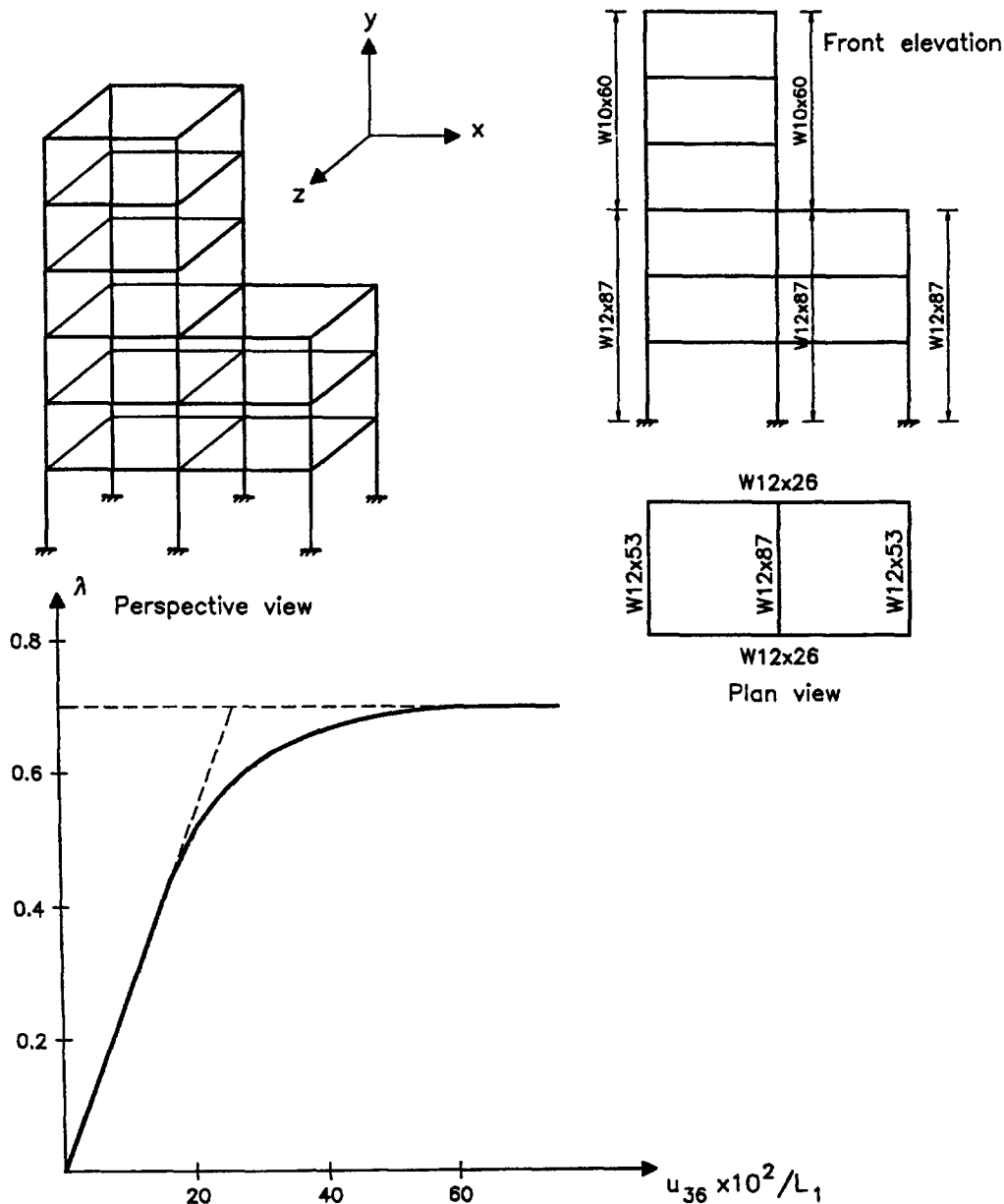


Fig. 2. Example 1. Six-storey space frame and the load-displacement curve.

**Table 1. Example 1. Characteristics of random variables**

Random variable	PDF	$\mu$	$\sigma$
Loads	Log- $N$	6.35	0.2

**Table 2. Example 1. Critical load factors for various plastic zone widths**

	$\epsilon_s = 0.005$	$\epsilon_s = 0.01$	$\epsilon_s = 0.02$	$\epsilon_s = 0.04$
$\lambda_c$	0.642	0.640	0.620	0.600

**Table 3. Example 1. Probability of failure for various plastic zone widths ( $\sigma_f = 0.10$ )**

Number of simulations	20	50	100	200	400
$\epsilon_s = 0.005$	0.10	0.079	0.07	0.076	0.075
$\epsilon_s = 0.010$	0.10	0.079	0.07	0.075	0.075
$\epsilon_s = 0.020$	0.20	0.160	0.15	0.140	0.130

**Table 4. Example 1. Probability of failure for various plastic zone widths ( $\sigma_f = 0.20$ )**

Number of simulations	20	50	100	200	400
$\epsilon_s = 0.005$	0.12	0.09	0.087	0.08	0.079
$\epsilon_s = 0.010$	0.12	0.09	0.085	0.08	0.080
$\epsilon_s = 0.020$	0.20	0.16	0.160	0.16	0.150

values of the loads and the modulus of elasticity. The type of probability density function (PDF), mean value and standard deviation used for the loads are shown in Table 1. Table 2 depicts the influence of the width between the two yield surfaces, used to define the yield zone, on the accuracy of the computed critical load factor. The tolerance criterion  $\epsilon_s$  controls the activation of a yield mode and may be considered as being proportional to the bandwidth of the yield zone. Tables 3 and 4 present the calculated probability of failure for

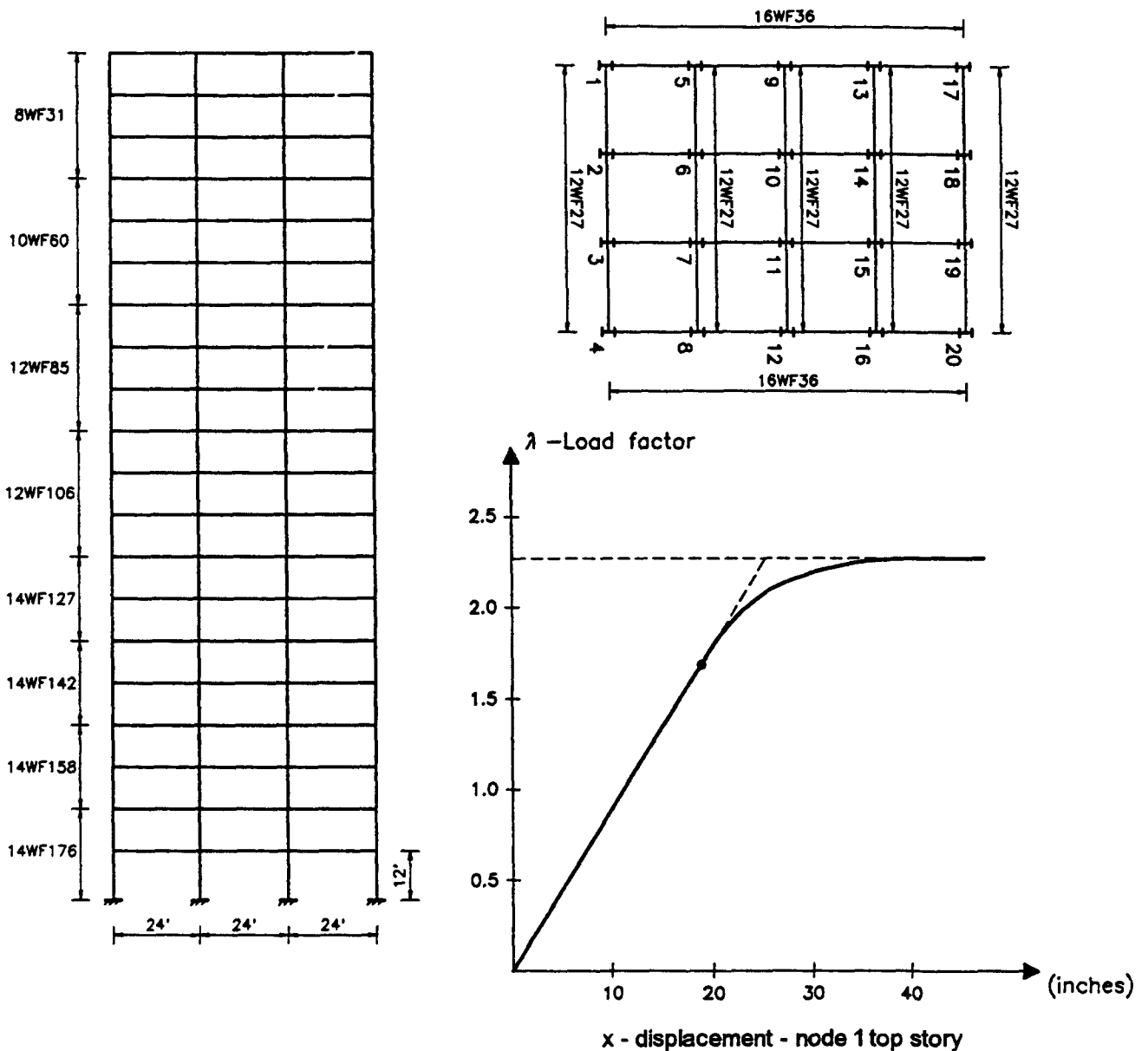


**Fig. 3. Example 2. Twenty-storey space frame and the load-displacement curve.**

**Table 5. Example 2. Characteristics of random variables**

Random variables	PDF	$\mu$	$\sigma$
Loads	Log- $N$	5.2	0.2

**Table 6. Example 2. Critical load factors for various plastic zone widths (\*Not converged due to spurious oscillations)**

	$\epsilon_s = 0.005$	$\epsilon_s = 0.01$	$\epsilon_s = 0.02$	$\epsilon_s = 0.04$
$\lambda_c$	*	2.25	2.15	0.190

**Table 7. Example 2. Critical load factors for different solution schemes**

	DIR	PCG ( $\epsilon = 10^{-1}$ )	PCG ( $\epsilon = 10^{-4}$ )
$\lambda_c$	2.25	2.26	2.25

**Table 8. Example 2. Probability of failure for different solution schemes ( $\sigma_f = 0.10$ ,  $\epsilon_s = 0.10$ )**

Number of simulations	20	50	100	200	400
DIR	0.07	0.10	0.09	0.075	0.074
PCG ( $\epsilon = 10^{-1}$ )	0.06	0.10	0.08	0.070	0.071
PCG ( $\epsilon = 10^{-4}$ )	0.07	0.10	0.09	0.077	0.076

**Table 9. Example 2. Probability of failure for different solution schemes ( $\sigma_f = 0.10$ ,  $\epsilon_s = 0.20$ )**

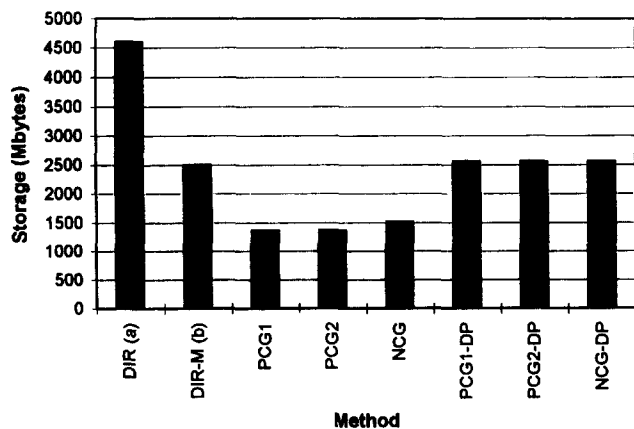
Number of simulations	20	50	100	200	400
DIR	0.10	0.14	0.12	0.088	0.089
PCG ( $\epsilon = 10^{-1}$ )	0.10	0.14	0.11	0.090	0.090
PCG ( $\epsilon = 10^{-4}$ )	0.10	0.14	0.12	0.088	0.089

various widths of the plastic zone and two different standard deviations of the stochastic field. From Tables 2–4 it can be observed that although the critical load factor appears to be less sensitive to the width of the plastic zone, this is not the case for the computed probability of failure. The latter, however, appears to be independent on the variability of the stochastic parameter of the modulus of elasticity. This can be explained by the fact that the variability of the modulus of

elasticity has marginal influence on the bearing capacity of the structures considered in this study. The complete Cholesky  $LDL^T$  factorization is used to solve the equations at each step, since this example is very small, to assess the efficiency of the solution schemes described in the previous section.

## Example 2

The second test example is the 20 storey space frame shown in Fig. 3. The mean loads considered here are uniform vertical forces applied at the joints and are equivalent to a uniform load of  $4.8 \text{ KNm}^{-2}$  and horizontal forces which are equivalent to a uniform pressure of  $0.956 \text{ KNm}^{-2}$  on the larger surface. The load–displacement curve for the mean values of the modulus of elasticity and the loads is also shown in Fig. 3. The number of equations is 1200 and the half bandwidth of the stiffness matrix is 65. The type of probability density function (PDF), mean value and standard deviation used for the loads are shown in Table 5. Tables 6 and 7 depict the influence of the width of the two yield surfaces, used to define the yield zone and that of the solution scheme used, on the accuracy of the computed critical load factor, respectively. The values of  $\epsilon$  correspond to the termination criterion of algorithm (20). Tables 8 and 9 present the computed probability of failure by different solution schemes for a variability of the modulus of elasticity 0.10, and widths of plastic zone  $\epsilon_s = 0.10$  and 0.20, respectively. The value of the parameter  $b_f$  was assumed to be 1. It can be observed that the accuracy of the solution is not influenced by the amount of the variability of the stochastic parameter or the solution scheme used but is only affected by the width of the plastic zone. Two PCG and one NCG versions are used in this example. PCG1 incorporates a tolerance criterion  $\epsilon = 0.1$ , PCG2 terminates when the normalized residual force vector becomes less than  $\epsilon = 0.01$ , while the NCG method is carried out with  $\epsilon = 0.1$ . The hybrid solution methods are implemented with mixed precision arithmetic in which all computations are performed in single precision, except for the double precision computation of the matrix–vector multiplication for the calculation of the residual vector. The updating of the preconditioning matrix is performed when the number of iterations exceeds 10 inside a load increment. This number is prescribed by the ratio of the computing time required for the factorization of the stiffness matrix over the time needed to perform one PCG iteration. Finally, the letter M after the abbreviated name of the direct method (DIR-M) stands for the modified factorization of the current elasto-plastic matrix. All PCG and NCG versions are implemented with the modified factorization. Figure 4 depicts the storage requirements for each of the above methods where the abbreviation DP denotes that all computations are performed in double

**Fig. 4. Example 2. Storage requirements of the solution methods.**



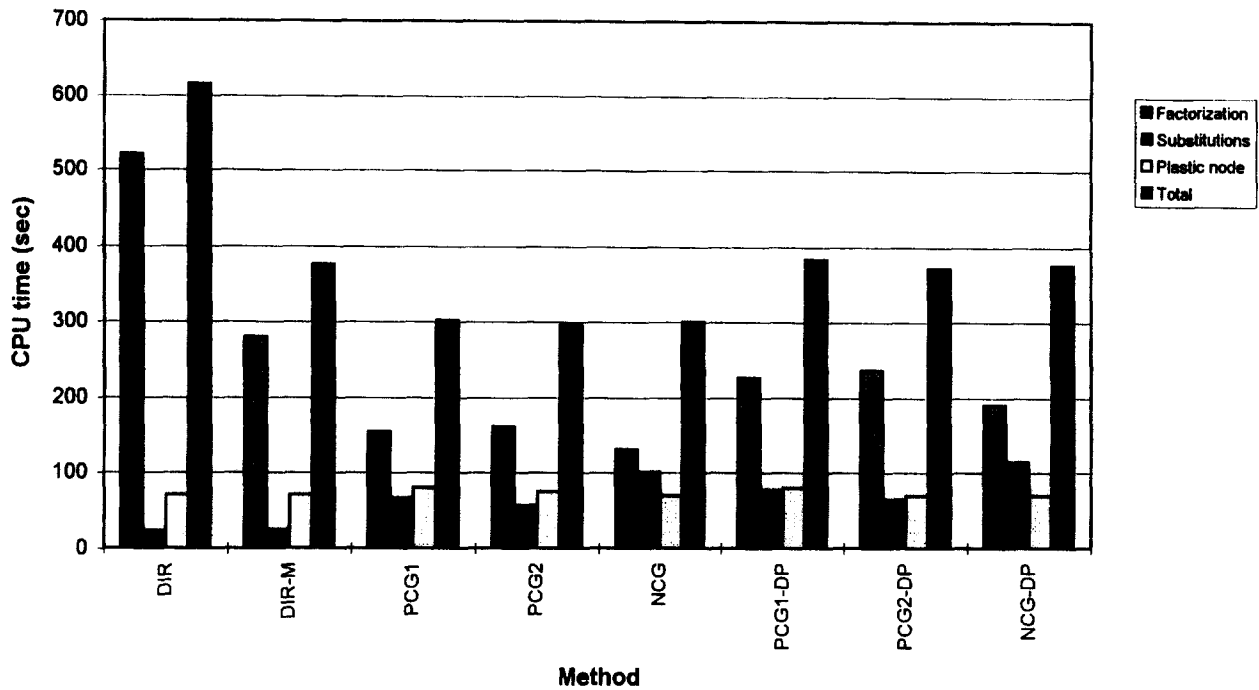


Fig. 5. Example 2. Average CPU time for three randomly selected simulations ( $\sigma_f = 0.10$ ).

precision arithmetic. Figure 5 shows the average performance of the methods for three randomly selected simulations when the standard deviation of the modulus of elasticity is taken as 0.10. The time entries are in seconds as obtained by the Silicon Graphics Indigo R4000 workstation. Figure 6 shows the number of conjugate gradient iterations required for PCG and NCG versions in one typical Monte Carlo simulation. Finally, Table 10 depicts the average critical load factors computed and the corresponding number of load steps of different solution schemes for three randomly selected simulations. It should be mentioned that the PCG1 method requires 10 additional load steps in order to reach the critical load factor. This indicates that the NCG method with the same tolerance is in general more robust compared to the corresponding PCG method.

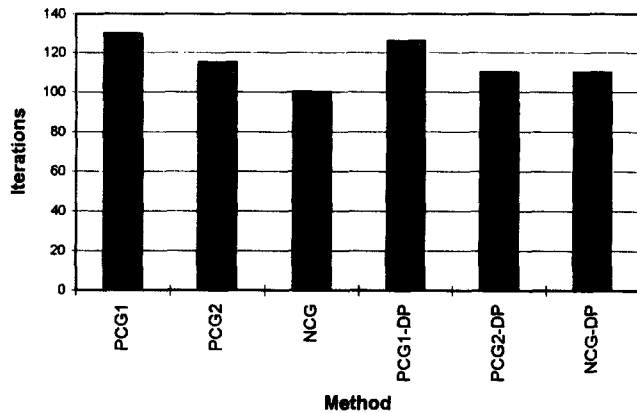


Fig. 6. Example 2. Number of conjugate gradient iterations in a typical Monte Carlo simulation ( $\sigma_f = 0.10$ ).

### 7 CONCLUSIONS

This paper presents a methodology for accurately and efficiently estimating the reliability of stochastic finite element systems with application to space frames. Accurate solutions of the step-by-step limit elasto-plastic analysis are obtained using the preconditioned conjugate gradient method and the Neumann conjugate gradient method in each Monte Carlo simulation, while significant reduction in computing time and storage requirements is achieved compared to the conventional direct method of solution. With the implementation of a plastic zone defined by the yield surface and a second surface, homothetic and close to the first one, the efficiency of the step-by-step incremental analysis is substantially improved. Small load steps or spurious oscillations of points around the corners of the yield surface are avoided, while simultaneous formation of more than one plastic node at each load step is accomplished. The use of a mixed precision arithmetic formulation for the preconditioned conjugate gradient method and the Neumann conjugate gradient method may substantially reduce the computer time and storage requirements without impairing the accuracy of the solution.

More specifically, the combination of a compact storage scheme for the stiffness matrix with the modified factorization procedure, in which alterations to the factorized matrix are confined to the bottom right-hand corner, appear to have a significant influence on the performance of the direct method. The storage requirements are reduced almost by half, while the computing time is less than 60% for the second example. The use of the complete factorized matrix as a preconditioner for

**Table 10. Example 2. Average critical load factors computed and the corresponding number of load steps for three randomly selected simulations and different solution schemes ( $\sigma_f = 0.10$ ,  $\epsilon_s = 0.01$ )**

Method	DIR	DIR-M	PCG1	PCG2	NCG	PCG1-DP	PCG2-DP	NCG-DP
Steps	70	70	80	67	70	80	67	70
$\lambda_c$	2.25	2.25	2.26	2.24	2.24	2.26	2.24	2.25

the PCG method produces a 25% reduction in computing time, with regard to the modified direct method. The improvement of the quality of the preconditioning matrix with a first-order Neumann series expansion of the inverse of the stiffness matrix, although it results in a reduction of 30% in the number of iterations compared to the PCG version, accomplishes a marginal improvement on the computing time. Nevertheless, it was found that the NCG method produces more robust results than the corresponding PCG method. The mixed precision implementation gives a 50% reduction in computer storage compared to the double precision implementation, while it requires 30% less computing time. It may, therefore, be concluded that the proposed PCG and NCG methods are superior compared to the conventional direct solution method for the stochastic finite element-based reliability analysis of large scale three-dimensional building frames using Monte Carlo simulation.

#### ACKNOWLEDGEMENTS

The authors would like to acknowledge the assistance of G. Deodatis in implementing the weighted integral method.

#### REFERENCE

- Shinozuka, M., Structural response variability. *J. Engng Mech.*, 1987, **113**, 825–842.
- Brener, C. E., Stochastic finite element methods — literature review. Internal Working Report No. 35-91, University of Innsbruck, Austria, 1991.
- Hisada, T. and Nakagiri, S., Stochastic finite element method developed for structural safety and reliability. *Proceedings of the 3rd Int. Conf. on Structural Safety and Reliability*, Trondheim, Norway, 1981, pp. 395–408.
- Liu, W., Mani, A. and Belytschko, T., Finite element methods in probabilistic mechanics. *Prob. Engng Mech.*, 1987, **2**(4), 201–213.
- Ghanem, R. G. and Spanos, P. D., *Stochastic Finite Elements: A Spectral Approach*. Springer Verlag, New York, 1991.
- Ghanem, R. G. and Spanos, P. D., Spectral stochastic finite element formulation for reliability analysis. *J. Engng Mech., ASCE*, 1991, **117**(10), 2351–2372.
- Shinozuka, M. and Deodatis, G., Response variability of stochastic finite element systems. *J. Engng Mech.*, 1988, **114**, 499–519.
- Deodatis, G., Weighted integral method I: stochastic stiffness matrix. *J. Engng Mech.*, 1991, **117**(8), 1851–1864.
- Yamazaki, F., Shinozuka, M. and Dasgupta, G., Neumann expansion for stochastic finite element analysis. *J. Engng Mech.*, 1988, **114**(8), 1335–1354.
- Papadrakakis, M. and Papadopoulos, V., Robust and efficient methods for the stochastic finite element analysis using Monte Carlo simulation. *Comp. Meth. in Applied Mechanics and Engineering*, 1996, **134**, 325–340.
- Deodatis, G., Stochastic FEM sensitivity analysis of nonlinear dynamic problems. *Prob. Engng Mech.*, 1989, **4**(3), 135–141.
- Wall, F. J. and Deodatis, G., Variability response function of stochastic plane stress/strain problems. *J. Engng Mech.*, 1994, **120**(9), 1963–1982.
- Shinozuka, M., Basic analysis of structural safety. *J. Struct. Engng, ASCE*, 1983, **109**, 721–739.
- Madsen, H. O., Krenk, S. and Lind, N. C., *Methods of Structural Safety*. Prentice-Hall, Englewood Cliffs, NJ, 1986.
- Thoft-Christensen, P., Reliability and optimisation of structural Systems '88. *Proceedings of the 2nd IFIP WG7.5*, London. Springer-Verlag, Berlin, 1988.
- Deodatis, G., and Shinozuka, M., Weighted integral method II: Response variability and reliability. *J. Engng Mech., ASCE*, 1991, **117**, 1865–1877.
- Spanos, P. D. and Brebbia, C. A., *Computational Stochastic Mechanics*. Computational Mechanics Publications, Elsevier, Southampton, 1991.
- Brener, C. E., On methods for nonlinear problems including system uncertainties. In *Structural Safety & Reliability*, ed. G. I. Schueller, M. Shinozuka and T. Yao, Balkema, Rotterdam, 1994, pp. 311–317.
- Ueda, Y. and Yao, T., The plastic node method: a new method of plastic analysis. *Comp. Meth. Appl. Mech. Engng*, 1982, **34**, 1089–1104.
- Papadrakakis, M. and Karamanos, S. A., A simple and efficient solution method for the limit elasto-plastic analysis of plane frames. *J. Comp. Mech.*, 1991, **8**, 235–248.
- Papadrakakis, M. and Papadopoulos, V., A computationally efficient method for the limit elasto-plastic analysis of space frames. *Comp. Mech. J.*, 1995, **16**(2), 132–141.
- Bitoulas, N. and Papadrakakis, M., An optimised computer implementation of the incomplete Cholesky factorization. *Comp. Systems in Engineering*, 1994, **5**, 265–274.
- Papadrakakis, M. and Bitoulas, N., Accuracy and effectiveness of preconditioned conjugate gradient method for large and ill-conditioned problems.

- Comp. Meth. Appl. Mech. Engng*, 1993, **109**, 219–232.
24. Shinozuka, M. and Deodatis, G., Simulation of stochastic processes by spectral representation method. *Appl. Mech. Rev.*, 1991, **44**, 191–203.
25. Papadrakakis, M., Papadopoulos, V. and Lagaros, N., Structural reliability analysis of elastic-plastic structures using neural networks and Monte Carlo simulation. *Comp. Meth. in Applied Mechanics and Engineering*, 1996, **136**, 145–163.
26. Orbinson, J. G., McGuire, W. and Abel, J. F., Yield surface applications in non-linear steel frames analysis. *Comp. Meth. Appl. Mech. Engng*, 1982, **33**, 557–573.

$$N_{35}^{(e)} = -x \left( 1 - \frac{x}{L^{(e)}} \right)^2$$

$$N_{39}^{(e)} = 3 \left( \frac{x}{L^{(e)}} \right)^2 - 2 \left( \frac{x}{L^{(e)}} \right)^3$$

$$N_{3,11}^{(e)} = -x \left[ -\frac{x}{L^{(e)}} + \left( \frac{x}{L^{(e)}} \right)^2 \right]$$

$$N_{44}^{(e)} = 1 - \frac{x}{L^{(e)}}, \quad N_{4,10}^{(e)} = \frac{x}{L^{(e)}}$$

The matrix containing the derivatives of the shape functions is given by

$$B^{(e)} = \begin{bmatrix} B_{11}^{(e)} & 0 & 0 & 0 & 0 & 0 & B_{17}^{(e)} & 0 & 0 & 0 & 0 & 0 \\ 0 & B_{22}^{(e)} & 0 & 0 & 0 & B_{26}^{(e)} & 0 & B_{28}^{(e)} & 0 & 0 & 0 & B_{2,12}^{(e)} \\ 0 & 0 & B_{33}^{(e)} & 0 & B_{35}^{(e)} & 0 & 0 & 0 & B_{39}^{(e)} & 0 & B_{3,11}^{(e)} & 0 \\ 0 & 0 & 0 & B_{44}^{(e)} & 0 & 0 & 0 & 0 & 0 & B_{4,10}^{(e)} & 0 & 0 \end{bmatrix}$$

**APPENDIX A**

**A.1 Stochastic element stiffness matrix of a 3-D beam element**

Using the standard displacement-based finite element analysis the matrix containing the shape functions for the 3-D beam element is given by

where

$$B_{11}^{(e)} = -\frac{1}{L^{(e)}}, \quad B_{17}^{(e)} = \frac{1}{L^{(e)}}$$

$$B_{22}^{(e)} = -\frac{6}{L^{(e)^2}} + \frac{12x}{L^{(e)^3}}, \quad B_{26}^{(e)} = -\frac{4}{L^{(e)}} + \frac{6x}{L^{(e)^2}}$$

$$N^{(e)} = \begin{bmatrix} N_{11}^{(e)} & 0 & 0 & 0 & 0 & 0 & N_{17}^{(e)} & 0 & 0 & 0 & 0 & 0 \\ 0 & N_{22}^{(e)} & 0 & 0 & 0 & N_{26}^{(e)} & 0 & N_{28}^{(e)} & 0 & 0 & 0 & N_{2,12}^{(e)} \\ 0 & 0 & N_{33}^{(e)} & 0 & N_{35}^{(e)} & 0 & 0 & 0 & N_{39}^{(e)} & 0 & N_{3,11}^{(e)} & 0 \\ 0 & 0 & 0 & N_{44}^{(e)} & 0 & 0 & 0 & 0 & 0 & N_{4,10}^{(e)} & 0 & 0 \end{bmatrix}$$

where

$$N_{11}^{(e)} = 1 - \frac{x}{L^{(e)}}, \quad N_{17}^{(e)} = \frac{x}{L^{(e)}}$$

$$N_{22}^{(e)} = 1 - 3 \left( \frac{x}{L^{(e)}} \right)^2 + 2 \left( \frac{x}{L^{(e)}} \right)^3$$

$$N_{26}^{(e)} = x \left( 1 - \frac{x}{L^{(e)}} \right)^2$$

$$N_{28}^{(e)} = 3 \left( \frac{x}{L^{(e)}} \right)^2 - 2 \left( \frac{x}{L^{(e)}} \right)^3$$

$$N_{2,12}^{(e)} = x \left[ -\frac{x}{L^{(e)}} + \left( \frac{x}{L^{(e)}} \right)^2 \right]$$

$$N_{33}^{(e)} = 1 - 3 \left( \frac{x}{L^{(e)}} \right)^2 + 2 \left( \frac{x}{L^{(e)}} \right)^3$$

$$B_{28}^{(e)} = \frac{6}{L^{(e)^2}} - \frac{12x}{L^{(e)^3}}, \quad B_{2,12}^{(e)} = -\frac{2}{L^{(e)}} + \frac{6x}{L^{(e)^2}}$$

$$B_{33}^{(e)} = -\frac{6}{L^{(e)^2}} + \frac{12x}{L^{(e)^3}}, \quad B_{35}^{(e)} = \frac{4}{L^{(e)}} - \frac{6x}{L^{(e)^2}}$$

$$B_{39}^{(e)} = \frac{6}{L^{(e)^2}} - \frac{12x}{L^{(e)^3}}, \quad B_{3,11}^{(e)} = \frac{2}{L^{(e)}} - \frac{6x}{L^{(e)^2}}$$

$$B_{44}^{(e)} = -\frac{1}{L^{(e)}}, \quad B_{4,10}^{(e)} = \frac{1}{L^{(e)}}$$

The deterministic matrices  $K_0^{(e)}$ ,  $\Delta K_0^{(e)}$ ,  $\Delta K_1^{(e)}$ ,  $\Delta K_2^{(e)}$  involved in eqn (5) are defined as follows:



where  $I_2 = E_0^{(e)} I_2^{(e)} / L^{(e)6}$ ,  $I_3 = E_0^{(e)} I_3^{(e)} / L^{(e)6}$  and  $L = L^{(e)}$

$$\Delta K_2^{(e)} = \begin{bmatrix} 0 & 0 & 0 & 0 & 0 & 0 & 0 & 0 & 0 & 0 & 0 & 0 \\ 144I_3 & 0 & 0 & 0 & 72I_3L & 0 & -144I_3 & 0 & 0 & 0 & 72I_3L \\ & 144I_2 & 0 & -72I_2L & 0 & 0 & 0 & -144I_2 & 0 & -72I_2L & 0 \\ & & 0 & 0 & 0 & 0 & 0 & 0 & 0 & 0 & 0 \\ & & & 36I_2L^2 & 0 & 0 & 0 & 72I_2L & 0 & 36I_2L^2 & 0 \\ & & & & 36I_3L^2 & 0 & -72I_3L & 0 & 0 & 0 & 36I_3L^2 \\ & & & & & 0 & 0 & 0 & 0 & 0 & 0 \\ \text{Symm.} & & & & & & 144I_3 & 0 & 0 & 0 & -72I_3L \\ & & & & & & & 144I_2 & 0 & 72I_2L & 0 \\ & & & & & & & & 0 & 0 & 0 \\ & & & & & & & & & 36I_2L^2 & 0 \\ & & & & & & & & & & 36I_3L^2 \end{bmatrix}$$

where  $I_2 = E_0^{(e)} I_2^{(e)} / L^{(e)6}$ ,  $I_3 = E_0^{(e)} I_3^{(e)} / L^{(e)6}$  and  $L = L^{(e)}$ .